Nanostructured High-Entropy Alloys with Multiple Principal Elements: Novel Alloy Design Concepts and Outcomes**

By *Jien-Wei Yeh,* Swe-Kai Chen, Su-Jien Lin, Jon-Yiew Gan, Tsung-Shune Chin, Tao-Tsung Shun, Chun-Huei Tsau,* and *Shou-Yi Chang*

For thousands of years the development of practical alloy systems has been based mainly on one principal element as the matrix, as in iron-based, copper-based, and aluminum-based alloys, and nickel-based superalloys, limiting the number of applicable alloy systems, even though a substantial amount of other elements is incorporated for property/processing enhancement.[1,2]

[*] *Prof. Jien-Wei Yeh, Prof. Su-Jien Lin, Dr. Jon-Yiew Gan, Prof. Tsung-Shune Chin*
Department of Materials Science and Engineering
National Tsing Hua University
Hsinchu 300, Taiwan
E-mail: jwyeh@mse.nthu.edu.tw
Prof. Swe-Kai Chen
Materials Science Center
National Tsing Hua University
Hsinchu 300, Taiwan
Prof. Tsung-Shune Chin
National United University
Miaoli 360, Taiwan
Dr. Tao-Tsung Shun
Materials Research Laboratory
Industrial Technology Research Institute
Chutung 310, Taiwan
Prof. Chun-Huei Tsau
Institute of Materials Science and Manufacturing
Chinese Culture University
Taipei 111, Taiwan
Prof. Shou-Yi Chang
Department of Materials Engineering
National Chung Hsing University
Taichung 402, Taiwan

[**] *The authors gratefully acknowledge the financial support for this research from the National Science Council of Taiwan under grants NSC-90-2218-E-007-054 and NSC-91-2120-E-007-007 and the Ministry of Economic Affairs of Taiwan under grant 92-EC-17-A-08-S1-0003. We also thank Professor Tung Hsu, Mr. Haesevoets, and Professor Theo Z. Kattamis for critically reading and editing the manuscript.*

Since the 1970s, metal-matrix composites and intermetallic compounds have attracted much attention.[3,4] In the former, the matrices are conventional alloys, particularly aluminum alloys. The latter are derived from Ti–Al, Ni–Al, and Fe–Al binary systems. During this time, new processing technologies such as rapid solidification and mechanical alloying have become popular.[5–7] These allow the exploration of new, enhanced performance alloys with fine microstructure, extended solubility, or even amorphous phases. All these alloy systems are based on one principal metallic element. In the last two decades, many researchers have explored a wide range of bulk amorphous alloys, including Pd-, Ln-, Zr-, Fe-, and Mg-based alloys.[7–14] The design concept of multi-component bulk amorphous alloys was, once again, based on one principal element.

The present study is focused on a new approach to alloy design with multiple principal elements in equimolar or near-equimolar ratios. Based on a general understanding of physical metallurgy and facts concerning binary and ternary phase diagrams, the formation of many intermetallic compounds using multiple principal elements may be anticipated.[15] Their complex microstructure is expected to result in brittleness, difficulty in processing, and challenging analysis. This expectation has discouraged alloy design with multiple principal elements. Nonetheless, solid solutions of many elements will tend to be more stable because of their large mixing entropies. Following Boltzmann's hypothesis on the relationship between entropy and system complexity,[16] the configurational entropy change per mole, ΔS_{conf}, during the formation of a solid solution from n elements with equimolar fractions may be calculated from the following equation.

$$\Delta S_{\text{conf}} = -k \ln w =$$

$$-R\,(1/n \ln 1/n + 1/n \ln 1/n + \cdots 1/n \ln 1/n) = -R \ln \frac{1}{n} = R \ln n \quad (1)$$

where k is Boltzmann's constant, w is the number of ways of mixing, and R is the gas constant: 8.314 J/K mole. As a result, for example, ΔS_{conf} for equimolar alloys with 3, 5, 6, 9, and 13 elements are 1.10R, 1.61R, 1.79R, 2.20R, and 2.57R, respectively. By Richards' rule,[16] the entropy changes in fusion of most metals are only empirically equal to R at their melting points. In comparison, equimolar alloys with three elements already have a ΔS_{conf} of 1.10R, larger than that of metal fusion, let alone those with five or more constituent elements. In fact, considering other positive contributions from factors such as vibrational, electronic, and magnetic moment randomness, the entropy change of mixing for equimolar alloys is even higher than that calculated.[16] Furthermore, if the formation enthalpies of two strong intermetallic compounds, such as NiAl and TiAl were divided by their respective melting points, the resulting ΔS_{conf}, 1.38R and 2.06R, are in the same range as the entropy changes of mixing in a system with more than five elements. This indicates that the tendency of ordering and segregation would be lowered by the high mixing entropy.[17] Consequently, alloys with a higher number of

 DOI: 10.1002/adem.200300567

principal elements will more easily yield the formation of random solid solutions during solidification, rather than intermetallic compounds, except for those with very large heats of formation, such as strong ceramic compounds: oxides, carbides, nitrides, and silicides.

In practice, to fully utilize the merit of high mixing entropy in the liquid- or solid-solution state, we define such high-entropy alloys (HE alloys) as those composed of five or more principal elements in equimolar ratios. In order to extend the scope of alloy design, HE alloys may contain principal elements with the concentration of each element being between 35 and 5 at.-%. Extensive trials have led to many alloy systems with simple crystal structures and extraordinary properties.[18,19]

Based on the experience with conventional alloys, a large number of intermetallics or other complex phases were expected to form in multi-element alloy systems.[15,20] However, the resultant phases in all investigated HE alloys were rather simple. Taking the as-cast $CuCoNiCrAl_xFe$ alloy system as an example, only very simple solid-solution structures, essentially bcc and fcc, were identified from the X-ray diffraction (XRD) patterns shown in Figure 1. Those alloys with aluminum contents from $x = 0$ to $x = 0.5$ showed a simple fcc structure. As x exceeded 0.8, a bcc structure appeared in addition to the fcc, and a spinodal decomposition occurred further on, leading to a modulated structure composed of ordered (B2) and disordered (A2) bcc phases, as confirmed by scanning electron microscopy (SEM), transmission electron microscopy (TEM) in Figure 2, and corresponding selected area diffraction (SAD) analyses. A single bcc structure was subsequently obtained for $x > 2.8$. Similar simple structures were also observed in other as-cast HE alloys with various contents of Cu, Co, Ni, Cr, or Fe. As a further example, a 10-element equimolar alloy, CuCoNiCrAlFeMoTiVZr, also exhibited a simple as-cast microstructure in which three main solid-solution phases were found, including two bcc phases (lattice constants 2.99 Å and 3.15 Å) and an amorphous phase. The superiority of simple solid solutions due to the aforementioned significant lowering of free energies by the high entropy of mixing

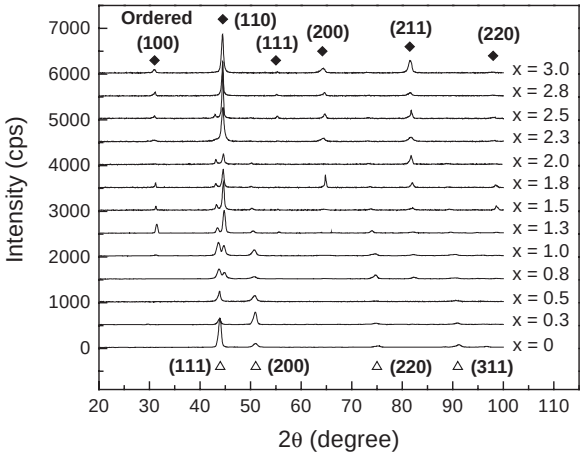

Fig. 1. XRD analyses of as-cast $CuCoNiCrAl_xFe$ alloy system with different x values: △, XRD peaks of fcc phase; ◆, XRD peaks of bcc phase.

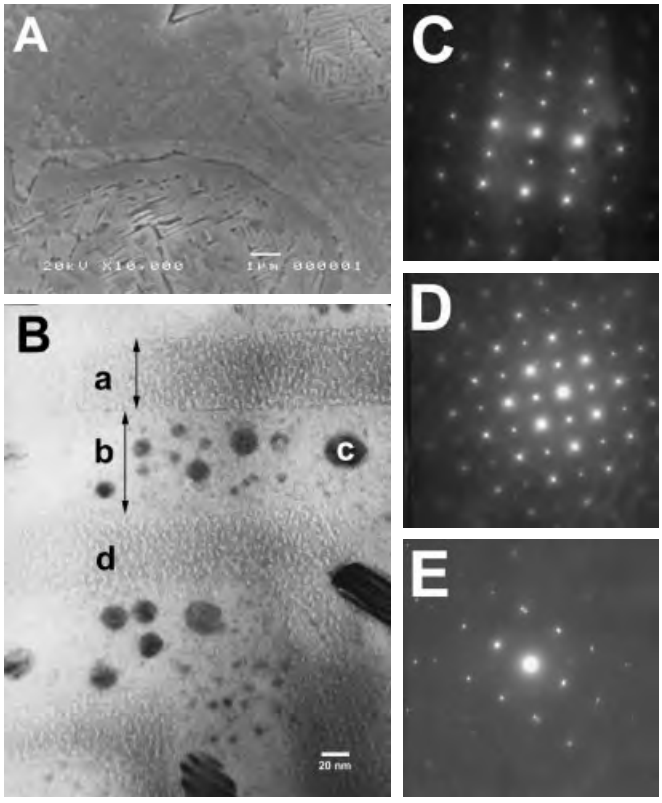

Fig. 2. Microstructures of as-cast CuCoNiCrAlFe alloy. A) SEM micrograph of etched alloy with dendrite (spinodal structure of disordered bcc and ordered bcc phases) and inter-dendrite (fcc phase) structures. B) TEM bright-field image; Ba, inter-spinodal plate, 70 nm wide, disordered bcc phase (A_2), lattice constant 2.89Å; Bb, spinodal plate, 100 nm wide, ordered bcc phase (B_2), lattice constant 2.89Å; Bc, nanoprecipitation in spinodal plate, 7 nm to 50 nm in diameter, close to fcc phase; Bd, nanoprecipitation in inter-spinodal plate, 3 nm in diameter, disordered bcc phase (A_2). C, D, and E, corresponding SAD patterns of B, Ba, and Bb with zone axes of bcc [011], bcc [001] + (010) superlattice, and fcc [011], respectively.

was thus manifest. The absence of complex phases or microstructures showed the significance of simple-structured HE alloys, whose development will further be encouraged.

It is expected that HE alloys might undergo phase transformations, such as spinodal decomposition, ordering, or precipitation during cooling, because of the importance of high mixing entropy in stabilizing solid solutions is reduced with decreasing temperature. However, from the viewpoint of kinetics, long-range diffusion for phase separation was sluggish in solid HE alloys that are devoid of a single principal matrix element. Difficulty in substitutional diffusion of elements in these alloys and interactions among interdiffusing species during partitioning lowered the rates of nucleation and growth, leading to the formation of ultrafine crystallites. As shown in Figure 2, the ultra-finely spaced and modulated structure of an as-cast CuCoNiCrAlFe equimolar alloy, resulted from spinodal decomposition within which crystallites precipitated at sizes of only several nanometers. In general, nanostructures were observed in the as-cast, homogenized, and even fully annealed states of HE alloys. On the contrary, similar nanocrystalline structures are rarely seen in the corresponding states of conventional alloys or bulk amorphous alloys, which require special heat treatments to produce nano-

sized precipitates.[2,21–23] We conclude, therefore, that HE alloys have a strong tendency to form microstructures consisting of simple matrices in which nanosized phases are dispersed.

As-cast HE alloys exhibited hardness values from 130 to 1100 H_V, depending on the alloy system. Table 1 shows nine typical alloy systems with hardness values higher than 590 H_V, and several commercial alloys for comparison purposes. Since in HE alloys there is no matrix element per se, all atoms may be regarded as solute atoms, and as a result the alloys form to a large extent saturated solid solution. A solid-solution strengthening effect impeding the motion of dislocations is therefore expected to enhance dramatically the strength of these alloys. Furthermore, the microstructural examination indicates that nanocrystallite dispersion would provide an effective precipitation strengthening. A nanospaced spinodal structure would also produce a nanocomposite strengthening effect. In some cases of the co-existence of an amorphous phase that is stronger than the crystalline one, the strength will be further increased. These multi-strengthening mechanisms are expected to be responsible, to different extents, for the high hardness values of HE alloys, as shown in Table 1.

Figure 3 shows the strong effect of aluminum concentration on the hardness of the $CuCoNiCrAl_xFe$ alloy system. A wide span of hardness values, from 133 to 655 H_V, was achieved depending on the x value. Since the $CuCoNiCrAl_xFe$ system has been identified as being composed of fcc and bcc solid solutions, the contribution of aluminum atoms

Table 1. Hardness of as-cast and fully annealed high-entropy alloys and commercial alloys. The high-entropy alloys exhibit very high hardness and excellent resistance to anneal softening even at 1000 °C for 12 h. Data scattering errors were within 3%.

Alloys	Hardness, HV as-cast	Hardness, HV annealed
CuTiVFeNiZr	590	600
AlTiVFeNiZr	800	790
MoTiVFeNiZr	740	760
CuTiVFeNiZrCo	630	620
AlTiVFeNiZrCo	790	800
MoTiVFeNiZrCo	790	790
CuTiVFeNiZrCoCr	680	680
AlTiVFeNiZrCoCr	780	890
MoTiVFeNiZrCoCr	850	850
316 Stainless Steel	189	155
17-4 PH Stainless Steel	410	362
Hastelloy C[a]	236	280
Stellite 6[b]	413	494
Ti-6Al-4V	412	341

[a] Ni–21.5Cr–2.5Co–13.5Mo–4W–5.5Fe–1Mn–0.1Si–0.3V–0.01C in wt.-%, [b] Co–29Cr–4.5W–1.2C in wt.-%

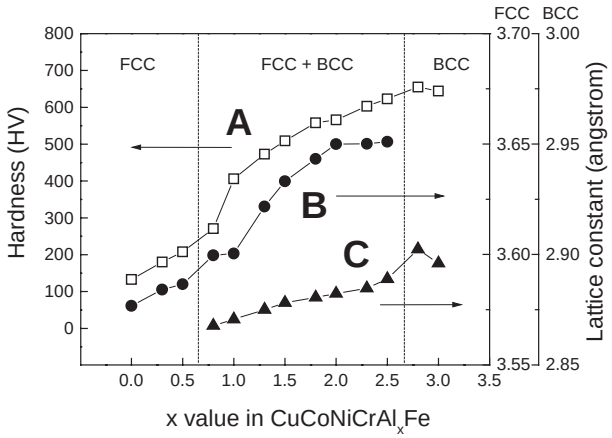

Fig. 3 Hardness and lattice constants of $CuCoNiCrAl_xFe$ alloy system with different x values: A) hardness of $CuCoNiCrAl_xFe$ alloys, B) lattice constant of fcc phase, C) lattice constant of bcc phase.

to the hardness of each phase must be related to a solution-hardening mechanism. It was apparent that aluminum not only had strong binding forces with other metallic atoms, but also a much larger atomic radius (1.4317 Å) than the others.[17,24–26] The increased tensile Young's modulus of $CuCoNiCrAl_xFe$ alloys with x value (114, 145, and 163 GPa for x = 0.5, 0.8, and 1.0, respectively) is a good evidence of the strong binding effect. The increase in lattice constant with increasing Al content indicates a corresponding larger lattice strain effect. Both binding energy and lattice strains are believed to be crucial to strengthening.

HE alloys were also found to exhibit excellent resistance to anneal softening. Table 1 shows that their hardness after annealing, even at 1000 °C for 12 h, remains almost the same in the as-cast condition, as is also the case for Ni-based Hastelloy and Co-based Stellite, which exhibit a lower hardness. Some HE alloys, especially those with an fcc structure, have the benefit of sustained high strength and extended ductility at elevated temperatures. The compressive yield strength of fcc $CuCoNiCrAl_{0.5}Fe$ alloy remained the same from room temperature up to 800 °C, as shown in Figure 4. Obvious bar-

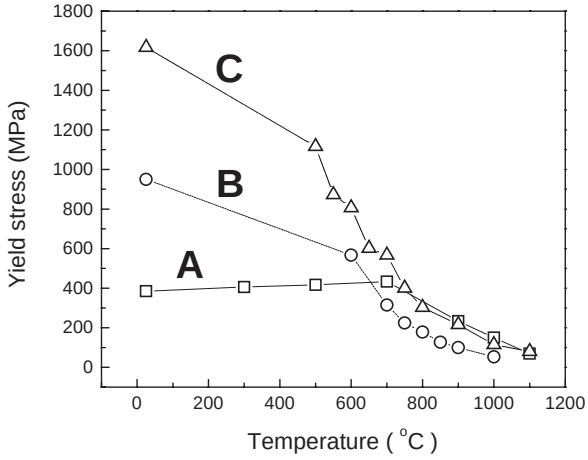

Fig. 4. Compressive yield strengths of $CuCoNiCrAl_xFe$ alloy system tested at different temperatures: A) $CuCoNiCrAl_{0.5}Fe$, B) $CuCoNiCrAl_{1.0}Fe$, C) $CuCoNiCrAl_{2.0}Fe$ alloys.

rel-shape deformation without fracture was observed after a compression leading to a significant reduction of 30% even at room temperature, stressing the high plasticity of this HE alloy. The combination of excellent stability, high-temperature strength, and ductility makes these alloys good candidates for high-temperature applications.

It was also found that the wear resistance of HE alloys was similar to that of ferrous alloys of the same hardness.[18,19] Furthermore, many of the HE alloys, especially those containing Cu, Ti, Cr, Ni, or Co, exhibited corrosion resistance as good as stainless steels, and the HE alloys containing Cr or Al demonstrated an excellent oxidation resistance, up to 1100 °C.[18,19] In addition to the ingot metallurgy route mentioned above, other processing technologies of rapid solidification, mechanical alloying, and thin-film coating deposition have also been applied to produce HE alloys with different features. These HE alloys also easily yielded a simple nanocrystalline matrix or an amorphous matrix, depending on their compositions and processing conditions. For instance, this is shown in Figure 5 where both the as-splat-quenched CuCoNiCrAlFeTiV foil and the as-sputtered $Cu_{0.5}$CoNiCrAl film consisted of a simple bcc structure. In Figure 5A the average grain size of the as-splat-quenched CuCoNiCrAlFeTiV foil is 0.8 μm, whereas that of the as-sputtered $Cu_{0.5}$CoNiCrAl film shown in Figure 5B is only 7 nm.

The promising properties of nanostructured HE alloys make them potentially suitable for many applications, such as tools, molds, dies, mechanical parts, and furnace parts that require high strength, thermal stability, and wear- and oxidation resistance. They also possess excellent corrosion resistance and can be used as anticorrosive high-strength materials in chemical plants, IC foundries, and even marine applications for piping, and pump components. In addition, coating technology will further expand the application of HE alloys to functional films, such as hard-facing of golf heads and rollers, diffusion barrier for Cu connections in ultralarge-scale integrated circuits, soft magnetic films for ultra-high-frequency communication. Most importantly, the tolerance to impurity elements of HE alloys is quite high, allowing their synthesis from recycled/scrapped metals in a cost effective, and environmentally sound fashion.

An arbitrary choice of a group of 13 mutually miscible metallic elements enables the design of 7099 HE alloy systems with 5 to 13 elements in equimolar ratios, such as CuCoNiCrAlFe

$$C_5^{13} + C_6^{13} + C_7^{13} + C_8^{13} + C_9^{13} + C_{10}^{13} + C_{11}^{13} + C_{12}^{13} + C_{13}^{13} = 7099 \quad (2)$$

where C_n^m is the number of combinations of m items taken n at a time. The huge number of alternatives considering the total 80 metallic elements in the periodic table may be easily imagined. Unequal mole alloys with minor alloying elements, such as $CuCo_{0.5}Ni_{1.2}CrAlFe_{1.5}Ag_{0.02}B_{0.1}C_{0.15}$ may be easily designed for further modification of processing and properties. As a result, HE alloys with multiple principal elements become countless in number, even after excluding chemically incompatible elements that produce liquid immiscibility. In contrast, there are only about 30 commonly used traditional alloy systems, including steels, aluminum alloys, and copper alloys. They have been thoroughly studied for centuries and reviewed in the 20-volume *ASM Metals Handbook*. It is recognized that their development was mature and nearly saturated at the end of the 20th century. Our new concept of HE alloys may lead to a new and uncharted territory, in which many possible new materials, new phenomena, new theories, and new applications are waiting to be discovered or created in the 21st century.

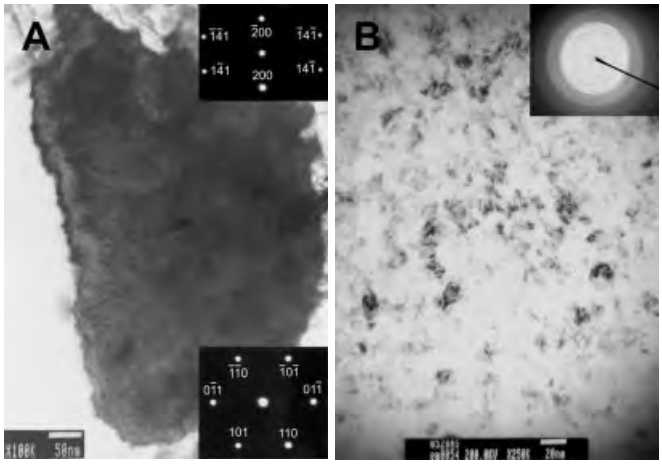

Fig. 5. TEM bright-field images and corresponding SAD patterns of high-entropy alloys: A) as-splat-quenched CuCoNiCrAlFeTiV foil with zone axes [014] and [$\bar{1}$11]; B) as-sputtered $Cu_{0.5}$CoNiCrAl film. Both alloys exhibited a simple solid-solution phase with a bcc crystal structure. The phase grain size in A was 0.8 μm, and the nanophase grain size in B, calculated from dark-field image, was about 7 nm.

Experimental

Fabrication of High-Entropy Alloys. The multiple principal element HE alloys in this study were prepared by arc melting the constituent elements at a current of 500 A in a cold copper hearth. The solidified ingots were approximately 50 mm in diameter and 20 mm thick. Melting and casting were performed at a pressure of 0.01 atm after purging with argon three times. Repeated melting for at least five cycles was carried out to improve chemical homogeneity of the alloy. Specimens (2.5 g) from the HE alloy ingots were re-melted, and splat-quenched at a cooling rate of 10^3–10^4 K/s, with a graphite hammer built inside the melting chamber, forming round foils about 200 μm thick. Cast HE alloy ingots were also machined to a thickness of 5 mm and used as sputtering targets. Thin films of the alloys were then deposited on silicon substrates by RF sputtering at a power of 80 W for 20 min at a pressure of 5 mTorr.

Microstructure Characterization. The ingots were sectioned, polished, and etched with aqua regia for observation under an optical microscope and a JEOL JSM-5410 SEM. Thin-foil specimens were prepared by mechanical thinning followed by ion milling, and subsequently were observed under a JEOL JEM-2010 TEM. A Rigaku ME510-FM2 X-ray diffractometer was used for identification of the crystalline structure. The typical radiation condition was 30 kV, 20 mA, Cu target, with the 2θ scan ranging from 20 to 100°, and performed at a speed of 1°/min.

Mechanical Property Evaluation. Hardness measurements of the alloys were conducted using a Vickers hardness tester (Matsuzawa Seiki MV-1) at a load of 49 N, and a speed of 70 μm/s for a loading time of 20 s. Seven indentations were performed and five medium data were averaged for each specimen. Scattering errors were within 3%. For high-temperature mechanical property tests, cast alloy specimens were prepared by vacuum induction melting, water-knife cut along the direction of thickness, and then polished to obtain cylinders of

10 mm diameter and 15 mm height. A Gleeble 2000 testing machine under a compression mode was used for these tests, which were conducted from room temperature to 1200 °C at a strain rate of 10^{-3}/s.

Received: December 01, 2003

[1] J. R. Davis (Ed.), *Metals Handbook*, 10th edn., Vol. 1, ASM International, Metals Park, OH, **1990**.

[2] J. R. Davis (Ed.), *Metals Handbook*, 10th edn., Vol. 2, ASM International, Metals Park, OH, **1990**.

[3] D. J. Lloyd, Ch. 13 in *Composites Engineering Handbook* (Ed: P. K. Mallick), Marcel Dekker, Inc., NY **1997**.

[4] J. H. Westbrook, in *Intermetallic Compounds: Principles and Practice* (Eds: J. H. Westbrook, R. L. Fleischer), Wiley, NY **1995**.

[5] J. R. Davis (Ed.), *Metals Handbook*, 10th edn., Vol. 7, ASM International, Metals Park, OH, **1990**.

[6] G. He, J. Eckert, W. G. Löser, L. Schultz, *Nature* **2003**, *2*, 33.

[7] A. Takeuchi, A. Inoue, *Mater. Trans.: JIM* **2000**, *41*, 1372.

[8] A. Inoue, in *Bulk Amorphous Alloys – Preparation and Fundamental Characteristics*, *Materials Science Foundations*, Vol. 4, Trans. Tech. Publications, Netherlands **1998**.

[9] H. W. Kui, A. L. Greer, D. Turnbull, *Appl. Phys. Lett.* **1984**, *45*, 615.

[10] A. Inoue, K. Ohtera, K. Kita, T. Masumoto, *Jpn. J. Appl. Phys.* **1988**, *27*, L2248.

[11] A. Inoue, T. Zhang, T. Masumoto, *Mater. Trans.: JIM* **1989**, *30*, 965.

[12] A. Inoue, T. Zhang, T. Masumoto, *Mater. Trans.: JIM* **1990**, *31*, 177.

[13] A. Peker, W. L. Johnson, *Appl. Phys. Lett.* **1993**, *63*, 2342.

[14] R. Akatsuka, T. Zhang, M. Koshiba, A. Inoue, *Mater. Trans.: JIM* **1999**, *40*, 258.

[15] A. Lindsay Greer, *Nature* **1993**, *366*, 303.

[16] R. A. Swalin, in *Thermodynamics of Solids*, 2nd edn. (Eds: E. Burke, B. Chalmers, J. A. Krumhansl), Wiley, NY **1991**, p. 21.

[17] F. R. de Boer, R. Boom, W. C. M. Mattens, A. R. Miedema, A. K. Niessen, Ch. 1 and Ch. 2 in *Cohesion in Metals: Transition Metal Alloys* (Eds: F. R. de Boer, D. G. Pettifor), Elsevier, NY **1988**.

[18] P. K. Huang, J. W. Yeh, T. T. Shun, S. K. Chen, *Adv. Eng. Mater.* **2004**, *6*, 74.

[19] C. Y. Hsu, J. W. Yeh, S. K. Chen, T. T. Shun, *Metall. Mater. Trans. A* **2004**, *4*, in press.

[20] H. Baker (Ed.), *Metals Handbook*, 10th edn., Vol. 3, ASM International, Metals Park, OH, **1992**.

[21] T. Zhang, A. Inoue, *Mater. Trans.: JIM* **1998**, *39*, 857.

[22] C. Fan, A. Takeuchi, A. Inoue, *Mater. Trans.: JIM* **1999**, *40*, 42.

[23] A. Inoue, *Acta. Mater.* **2000**, *48*, 279.

[24] H. Bakker, in *Enthalpies in Alloys*, *Materials Science Foundations*, Vol. 1, Trans. Tech. Publications, Netherlands **1998**.

[25] International Union of Crystallography, *International Tables for X-ray Crystallography*, Kynock Press, Birmingham, UK **1968**.

[26] J. L. C. Daams, P. Villars, J. H. N. van Vucht, in *Atlas of Crystal Structure Types for Intermetallic Phases*, Vol. 1, ASM International, Metals Park, OH **1991**.

Hypereutectic Al-Si Binary Alloys Prepared by Melt Spinning Method

By *Z. K. Zhao*, *J. C. Li*, and *Q. Jiang**

Since Al-base amorphous alloys with high tensile strength above 1000 MPa were found in 1988,[1] non-equilibrium Al-base alloys have attracted great attention.[2–10] Recently, it is further found that the alloys whose structures consist of amorphous phases and nanocrystals process a better mechanical property than a single amorphous alloy or a single nanostructured alloy[6,8,10] since the mixed-structured alloys have both high strength induced by nanocrystals and good plasticity due to appearance of amorphous alloys.

Although an Al-Si binary alloy has wide industrial application with lower cost, it has not been paid great attention since the eutectic Al-Si alloy has a bad glass forming ability (GFA) while a eutectic alloy should have the best GFA among the alloy system due to its lowest melting point. Although ternary Al-Fe-Si, Al-Fe-Ge and Al-Mn-Si alloys have amorphous structure by the melt-spun technique,[11,12] the structures of binary Al-Si[13] and Al-Ge[14] alloys through a gun quenching technique are mixtures of amorphous and crystalline phases where the amorphous phase is unstable and crystallize even at room temperature. However, according to a polymorphous diagram of Al-Si system, which is schematically shown in Figure 1, when the composition range of Si% (atom percentage) is located between 25 % and 45 %, glass may be formed from liquid with a high cooling rate[15–16] where the polymorphous crystallization is absent. The model

[*] *Prof. Z. K. Zhao, Prof. J. C. Li, Prof. Q. Jiang*
Key Laboratory of Automobile Materials
Ministry of Education
and Department of Materials Science & Engineering
Jilin University, Changchun 130025 (China)
E-mail: jiangq@jlu.edu.cn
Prof. Z. K. Zhao
Department of Materials Science & Engineering
Changchun University of Technology
Changchun 130012 (China)

[**] *The authors gratefully acknowledge the financial support of NNSFC under Grant (50025101)*

